Color Stabilization of Malvidin 3-Glucoside: Self-Aggregation of the Flavylium Cation and Copigmentation with the *Z*-Chalcone Form

Chantal Houbiers,[†] João C. Lima,[†] António L. Maçanita,*[,†,‡,§] and Helena Santos*[,†,⊥]

Instituto de Tecnologia Química e Biológica, Universidade Nova de Lisboa, Apt. 127, 2780 Oeiras, Portugal, and Instituto Superior Técnico, Av. Rovisco Pais, 1096 Lisboa codex, Portugal

Received: July 16, 1997; In Final Form: February 3, 1998

^{1}H NMR spectroscopy was used to characterize the aggregation processes leading to color stabilization of the natural anthocyanin, malvidin 3-glucoside. The concentrations of the different forms in aqueous solution were determined as a function of pH for several values of the total anthocyanin concentration. The chemical shifts were measured as a function of total concentration and temperature, and the concentration dependence of the T_1 values of relevant resonances were determined for different concentrations and pH values. The data are in agreement with a model that considers the occurrence of multimeric aggregates of flavylium cations at very acidic pH and copigmentation of flavylium cations with the *Z*-chalcone form at moderately acidic pH. The following equilibrium constants were determined: $K_h = 0.0016$ M for the flavylium cation hydration, $K_T = 0.26$ for the hemiacetal/*E*-chalcone tautomerism, $K_i = 0.6$ for the *E*-chalcone/*Z*-chalcone isomerization, $K = 3700$ M^{-1} for the flavylium cation self-aggregation, and $K' = 3080$ M^{-1} for the flavylium cation/*Z*-chalcone copigmentation. The relevance of these results for color enhancement is discussed.

Introduction

Malvidin 3-glucoside is a water-soluble natural pigment, belonging to the group of anthocyanins which play an important role in the coloring of fruits and flower petals. These compounds are potentially very interesting as natural colorant additives in foods, but this application requires improvement of their chemical and photochemical stability.[1] Therefore, it is important to study anthocyanin stability in aqueous solution. The structural changes occurring in aqueous solutions in the pH range 2−5 have been investigated by Brouillard et al.[2,3] In the particular case of malvidin 3-glucoside, the quinonoidal base (A), hemiacetal (B), and chalcone (C) forms were detected in addition to the flavylium cation (AH^+).[4,5] Interconversion between these structures takes place according to the scheme in Figure 1. Deprotonation of the flavylium cation leads to three quinonoidal basic forms, whereas hydration of the flavylium cation leads to two colorless hemiacetal forms, which can convert to a *E*-chalcone isomer (C_E) upon opening of the pyrylium ring. This chalcone isomer is in slow (in the NMR time scale) exchange with the *Z*-chalcone isomer (C_Z). At pH lower than 3, the colored flavylium cation is prevailing, while at increased pH values the colorless hemiacetal and chalcone forms appear, resulting in bleaching. Thus, at moderately acidic pH values the color is lost, unless a mechanism for color stabilization exists. Several mechanisms for color stabilization, involving formation of molecular complexes, have been proposed.[6] Formation of complexes competes with the nucleophilic attack of water onto the colored form, thus restoring color. One way of stabilizing color is by self-association of the colored flavylium cations or anhydrobases, thereby preventing the nucleophilic attack of water. Self-association was suggested first by Asen et al.,[7] based on the observation that the color intensity increased manyfold, upon increasing the concentration. Hoshino et al. demonstrated self-association of flavylium cations or quinonoidal bases by means of circular dichroism and by ^{1}H NMR measurements.[8−12] In the analysis of the NMR data, these authors took advantage of the observation that the chemical shifts of the aromatic protons move upfield with an increase in pigment concentration, to propose the existence of vertical stacking of the molecules caused by hydrophobic interaction between aromatic rings.[10] These authors determined self-association constants[11,12] based on the equation of Dimicoli and Hélène.[13] Self-association of the anthocyanin petanin was also demonstrated from measurements of intermolecular nuclear Overhauser enhancement effects in 2D NOESY spectra.[14,15]

An alternative process leading to color stabilization is designated copigmentation in which the association between the colored form and a colorless molecule (copigment) prevents the otherwise more favorable process of hydration of the colored form.[16,17] Copigmentation involving other polyphenols is now believed to be one of the most efficient processes allowing color stabilization in vivo. Finally, intramolecular copigmentation can also occur in anthocyanins such as those possessing cinnamic residues linked to glucosyl moieties (also called intramolecular sandwich-type stacking[18]). These molecules exhibit deep stable colors at neutral pH.[19−21]

In this study, NMR was used to characterize the aggregation processes leading to color stabilization of the natural anthocyanin, malvidin 3-glucoside.

Experimental Section

Sample Preparation. Malvidin 3-glucoside was purchased from Extrasynthese S.A. (France) and used without further purification. The compound was freeze-dried once from ^2H_2O and dissolved in ^{2}HCl (approximately 0.1 M). Final pH was

† Universidade Nova de Lisboa.
‡ Instituto Superior Técnico.
§ E-mail: santos@itqb.unl.pt.
⊥ E-mail: macanita@itqb.unl.pt.

S1089-5647(97)02320-1 CCC: $15.00
Published on Web 04/08/1998

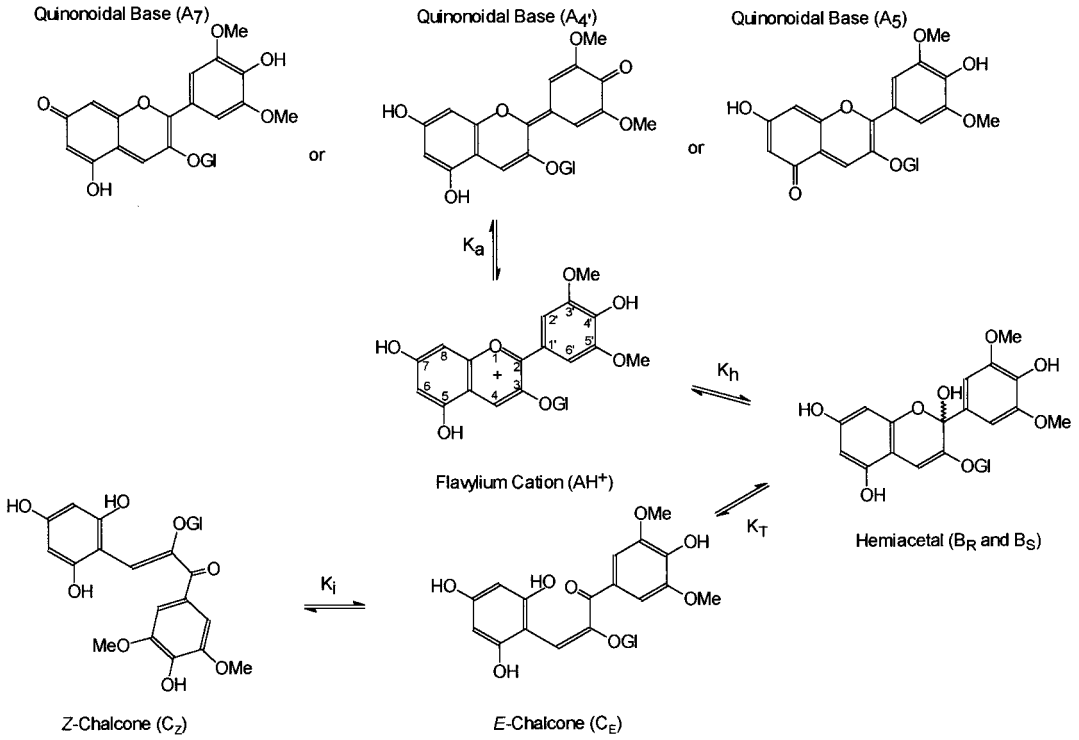

Figure 1. Structures and interconversion pathways between the various forms of malvidin 3-glucoside. In the structures Gl stands for the glucosyl moiety.

typically 0.7 and was changed by the addition of NaO^2H. Samples were allowed to equilibrate for at least 6 h. Concentrations were determined using $\epsilon = 27\,000\ M^{-1}\ cm^{-1}$ for the extinction coefficient at 518 nm of the flavylium form after appropriate dilution ($\epsilon[AH^+] < 1$) at acidic pH (<1). Quoted pH values are direct meter readings without correction for isotopic effects.

UV−Vis Absorption Spectra. Absorption spectra of concentrated solutions of malvidin 3-glucoside were run in an OLIS-15 spectrophotometer using cells with a 0.5-mm optical path.

NMR Spectroscopy. ^1H NMR spectra were obtained in Bruker AMX-300 or Bruker AMX-500 spectrometers, operating at 300.13 and 500.13 MHz, respectively. The spectra were run with water presaturation and are referenced to internal 3-(trimethylsilyl)propanesulfonic acid at 0 ppm. For quantitative measurements, spectra were acquired with a recycle delay of 8 s and a flip angle of 60° in order to ensure full relaxation of the resonances due to malvidin 3-glucoside and lactate. The resonance of lactate was used as an intensity standard for quantification.

NOE difference spectra were acquired with a total recycle delay of 4.5 s, with alternation between off-resonance and on-resonance irradiation every 16 scans. The delay for selective irradiation was 1.5 s. The experiments were performed with a 1.5 mM solution at pH 3.2. T_1 experiments were performed with the standard inversion recovery pulse sequence, using a total recycle time of at least 9 s. T_1's were determined from the fitting of peak heights to a single-exponential function. Unless otherwise stated, all spectra were run at 298 K.

Fitting Methods. The curves representing the pH dependence of the molar fractions of the different species were fitted to the derived theoretical equations by using the multiparametric minimization routine (fmins) of the AT-Matlab package (The Mathworks Inc.).

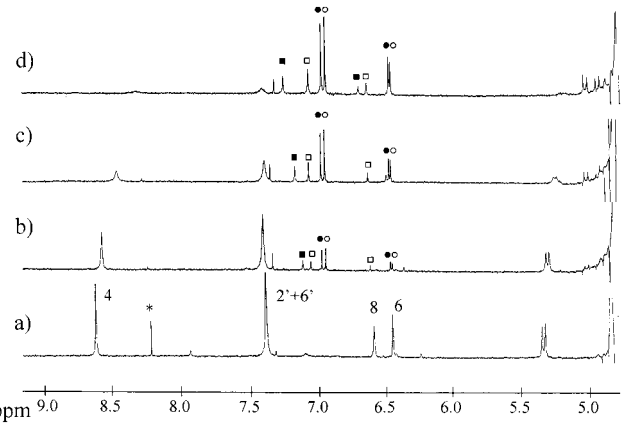

Figure 2. ^1H NMR spectra of malvidin 3-glucoside in ^2H_2O at different pH's, $T = 298$ K, and total concentration 0.68 mM: (a) pH 0.76, (b) pH 2.66, (c) pH 3.34, (d) pH 4.24. The flavylium cation peaks are labeled according to their specific assignments in spectrum a. The peaks of the remaining forms are labeled in spectrum d with the symbols: (○/●) R/S hemiacetal; (□) *E*-chalcone; (■) *Z*-chalcone; (*) nonassigned impurity from DCl.

Results and Discussion

Dependence of Molar Fractions on pH. The pH dependence of the proton NMR spectra of malvidin 3-glucoside at 298 K was determined for three different concentrations (0.14, 0.42, and 0.68 mM). Figure 2 illustrates the results obtained with the highest concentration solution. Assignment of resonances due to protons 2′, 6′, and 4 in the five different forms (flavylium, R/S hemiacetals, *E*- and *Z*-chalcone) is straightforward by comparison with published spectra of malvidin 3,5-diglucoside.[22] Protons 6 and 8 exchange with deuterium in the solvent, the corresponding resonances disappearing from the spectrum a few hours after sample preparation. Resonance intensities were measured as a function of pH, and the molar fractions of the different forms were calculated (Figure 3). The sum of intensities is independent of pH for a given initial

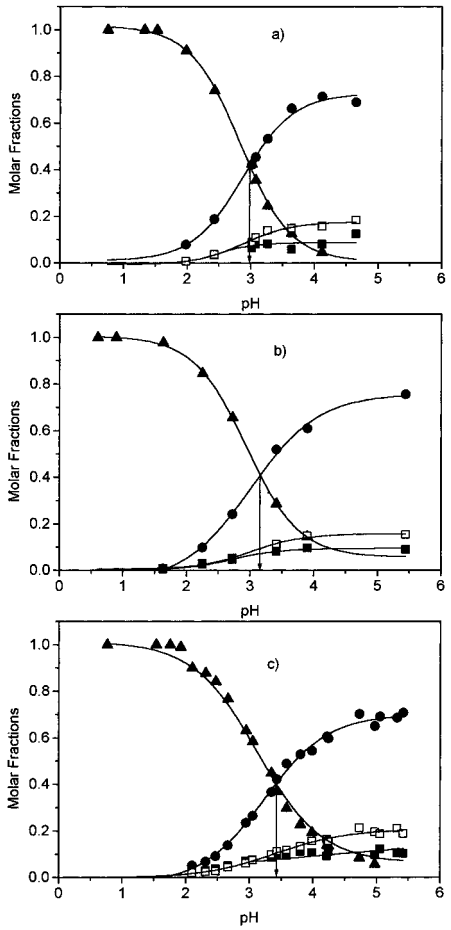

Figure 3. Plot of the molar fractions of the different forms of malvidin 3-glucoside determined by NMR as a function of pH for three different total concentrations: (a) 0.14 mM, (b) 0.42 mM, (c) 0.68 mM. The different forms are labeled as follows: flavylium cation (▲), sum of the hemiacetal forms (●), *E*-chalcone (□), *Z*-chalcone (■). The lines are best fits with $K_h = 0.0016$, $K_T = 0.26$, $K_i = 0.6$ and the concentration dependent values of K_d and K_{cop} shown in Table 2 (see text). $T = 298$ K.

concentration. From these plots the value of the equilibrium constant for the interconversion between the flavylium cation and the hemiacetal forms, K_h, appears to be concentration dependent, which means that this is an apparent equilibrium constant here designated as K_h^{app}. This apparent concentration dependence of K_h^{app} is explained by the occurrence of aggregation of the flavylium cation (see below).

Dependence of Chemical Shifts on pH. The pH dependence of the chemical shift of the resonance due to H_4, in the different forms of malvidin 3-glucoside (flavylium, two hemiacetal forms, *E*- and *Z*-chalcone), are shown in Figure 4 for the three different concentrations examined. Similar plots were obtained for the chemical shifts of resonances $H_{2'} + H_{6'}$ (not illustrated). The H_4 chemical shifts in the flavylium cation and *Z*-chalcone forms depend on the total malvidin 3-glucoside concentration, in contrast with the observation for the hemiacetals and *E*-chalcone forms whose chemical shifts are concentration independent. At very acidic pH (near pH 1), the H_4 resonance relative to the flavylium form shifts from 8.84 ppm (at 0.14 mM, Figure 4a), to 8.62 ppm (at 0.68 mM, Figure 4c). Since at such pH values the flavylium cation is the only species in solution, this concentration dependence of chemical shifts indicates the occurrence of self-association.

Interestingly, when the flavylium and the *Z*-chalcone forms coexist (pH 2.5−4.5; see Figure 3), a strong dependence of the

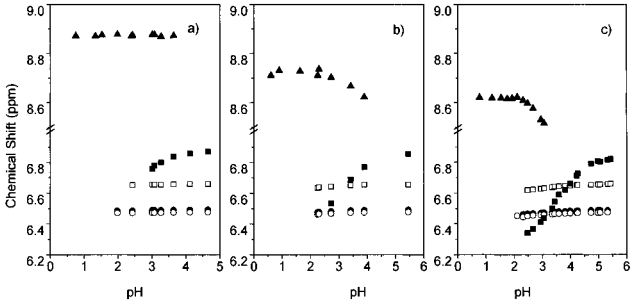

Figure 4. Plot of the chemical shifts of proton H_4 in the different forms of malvidin 3-glucoside as a function of pH, for three values of total concentration, at $T = 298$ K: (a) 0.14 mM, (b) 0.42 mM, (c) 0.68 mM. Symbols: flavylium cation (▲), hemiacetal forms (○/●), *E*-chalcone (□), *Z*-chalcone (■).

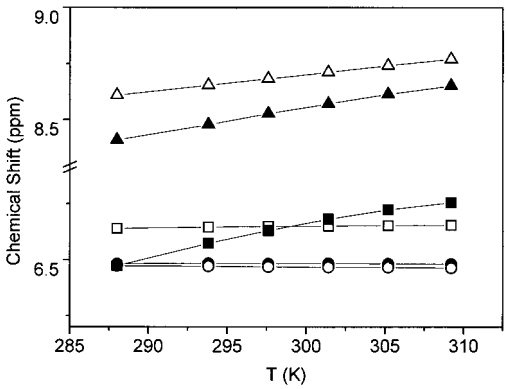

Figure 5. Plot of the temperature dependence of the chemical shifts of proton H_4 in the different forms of a 0.66 mM solution of malvidin 3-glucoside at pH 0.6, flavylium (Δ); at pH 3.5, flavylium (▲), hemiacetal forms (○/●), *E*-chalcone (□) , *Z*-chalcone (■).

Z-chalcone chemical shift is observed not only with concentration but also with pH (Figure 4). Furthermore, at pH values above 4.5, where the concentration of the flavylium form is negligible, the chemical shift of H_4 in the *Z*-chalcone becomes independent of the solution concentration and of pH. In fact, the chemical shift of H_4 in the flavylium form decreases with pH in response to increasing concentrations of the *Z*-chalcone form. Reciprocally, the *Z*-chalcone chemical shift increases and levels off at a maximum value in response to the decrease in the flavylium concentration at higher pH. These results strongly support the hypothesis that a complex is formed between *Z*-chalcone and flavylium. The analysis of the chemical shifts due to resonances 2′, and 6′ leads to similar conclusions (not shown).

Dependence of Chemical Shifts on Temperature. The temperature dependence of proton chemical shifts for a 0.66 mM malvidin 3-glucoside solution at two pH values are shown in Figure 5. At pH 0.6 only flavylium is present, but at pH 3.5 all forms are present. Flavylium and *Z*-chalcone resonances show a shift to higher frequency upon increasing the temperature, whereas resonances due to hemiacetal forms and *E*-chalcone do not shift significantly with temperature (Figure 5). This result further supports the hypothesis for association between the *Z*-chalcone and flavylium forms, a process not favored by an increase in temperature, as expected for an exothermic process. The effect of temperature on the chemical shift of the flavylium H_4 at pH 0.6, where only self-association of flavylium can occur, is smaller than that observed at the higher pH value (3.5), where there is an additional contribution from copigmentation with *Z*-chalcone.

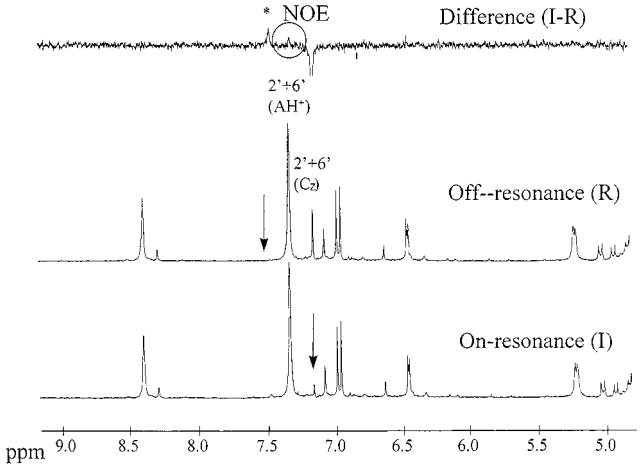

Figure 6. NOE difference experiment: (I) spectrum with irradiation of the 2′,6′-proton resonance of *Z*-chalcone; (R) spectrum with blank irradiation. The difference spectrum is shown on top (I−R): pH = 3.2, T = 308 K, C_o = 1.5 mM. The arrows indicate the irradiation position.

TABLE 1: T_1's (in seconds) of H_4 Protons in the Different Forms of Malvidin 3-Glucoside, at T = 298 K, as a Function of pH and Total Concentration, C_0

pH	$C_0/10^{-3}$ M	AH^+	B	C_E	C_Z
0.80	0.14	1.02			
	0.67	0.93			
3.35	0.12	0.49	1.36	1.30	0.94
	1.1	0.30	1.33	1.25	0.55

NOE Experiments. Information on geometric relationships in the complex flavylium/*Z*-chalcone was sought from measurements of the nuclear Overhauser effect (NOE) at pH 3.2. Upon irradiation of the $H_{2'+6'}$ resonance of *Z*-chalcone, a small positive NOE was observed on the $H_{2'+6'}$ resonance in the flavylium form (Figure 6).

T_1 Measurements. T_1's for resonances H_4 and $H_{2'+6'}$ were measured for the different forms of malvidin 3-glucoside for different concentrations, at pH 0.8 (when only flavylium is present) and at high pH (3.3), where all forms are present. The results are summarized in Table 1. At the lower pH, T_1's of resonances in the flavylium form slightly decrease (by 9%) when the concentration is increased. At high pH, the T_1's in the hemiacetals and *E*-chalcone forms are constant in the concentration range examined, while T_1's of flavylium and *Z*-chalcone both decrease by 40%. This large decrease in T_1's for flavylium and *Z*-chalcone further support the existence of association between flavylium and *Z*-chalcone. Complexation between the cyanin flavylium cation and several chalcones has been previously proposed by other authors.[23]

UV−Vis Absorption Spectra. Absorption spectra of diluted (1×10^{-5} M) and concentrated (0.42 and 0.68 mM) aqueous solutions of malvidin 3-glucoside at pH = 0.7 are shown in Figure 7. The clear band broadening and decrease of the apparent molar extintion coefficient ($\epsilon^{max}(1 \times 10^{-5}$ M) = 2.7×10^4 L mol^{-1} cm^{-1}, $\epsilon^{max}(0.42$ mM) = 2.2×10^4 L mol^{-1} cm^{-1}, and $\epsilon^{max}(0.68$ mM) = 2.1×10^4 L mol^{-1} cm^{-1}) as a function of concentration is typical of a sandwich-type aggregation process leading to exciton splitting.[24]

Model and Data Analysis

From the results and discussion presented above, the following initial assumption for the analysis of the multiequilibria of malvidin 3-glucoside (eqs 1−5) was considered: the aggregation

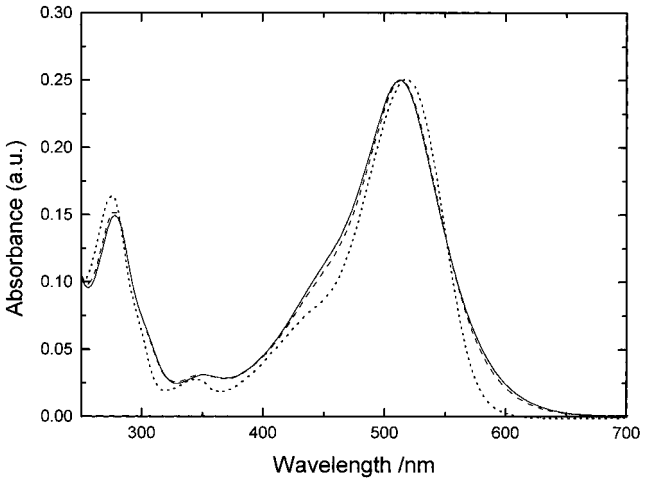

Figure 7. UV−vis absorption spectra of malvidin 3-glucoside in aqueous acid solution (pH = 0.7): (—) 0.68 mM, (- - -) 0.42 mM, (···) 1×10^{-5} M. The spectra are normalized at the maximum of the lower energy absorption band. Apparent extinction coefficients ϵ^{max} (L mol^{-1} cm^{-1}) are: (0.68 mM) 2.1×10^4, (0.42 2.2×10^4, (1×10^{-5} M) = 2.7×10^4.

reaction is a dimerization and the stoichiometry of the flavylium−chalcone copigment is 1:1.

$$2AH^+ \overset{K_d}{\rightleftharpoons} D \quad (1)$$

$$AH^+ \overset{K_h}{\rightleftharpoons} B + H^+ \quad (2)$$

$$B \overset{K_T}{\rightleftharpoons} C_E \quad (3)$$

$$C_E \overset{K_i}{\rightleftharpoons} C_Z \quad (4)$$

$$AH^+ + C_Z \overset{K_{cop}}{\rightleftharpoons} AHC_Z^+ \quad (5)$$

AH^+ represents the flavylium cation, D is the product of dimerization of flavylium, B is the hemiacetal form, C_E is the *E*-chalcone form, C_Z is the *Z*-chalcone form, AHC_Z^+ is the product of flavylium cation copigmentation with the *Z*-chalcone form, and K_d and K_{cop} are the dimerization and copigmentation equilibrium constants, respectively. The formation of quinonoidal bases was not included because there is no evidence for its presence in the UV/vis absorption spectra at pH values lower than 4.5. Also, the hydration of both complexes, D and AHC_Z^+, is neglected. This seems to be a reasonable approximation because the hydration constants of the complexes must be significantly smaller than K_h. However, it restricts the meaning of the values of K_d and K_{cop}, which under these conditions are lower limit approximations to the exact K_d and K_{cop} values.

Determination of K_d from Chemical Shifts as f(pH). The chemical shifts of the proton resonances of the flavylium form were measured as a function of concentration in the range 0.009 to 2.2 mM at pH 0.8. As the concentration increases, the aromatic protons shift to lower frequency. The self-association constant for flavylium was determined by the methodology proposed by Dimicoli and Hélène[13], according to eq 6.

$$\left(\frac{\delta\sigma}{C_0}\right)^{1/2} = \left(\frac{2K_d}{\delta\sigma_{C_2}}\right)^{1/2}(\delta\sigma_{C_2} - \delta\sigma) \quad (6)$$

in which K_d is the dimerization constant, C_0 is the total concentration of pigment, $\delta\sigma$ is the difference between extrapo-

lated chemical shift at infinite dilution and actual chemical shift at a given concentration, $\delta\sigma_{C_2}$ is the difference between the chemical shift of the dimer and the actual chemical shift.

In a plot of $(\delta\sigma/C_0)^{1/2}$ vs $\delta\sigma$, K_d can be calculated from the *x*-axis intercept ($\delta\sigma_{C_2}$) and the slope $(2K_d/\delta\sigma_{C_2})^{1/2}$. A value of $K_d = 1800 \pm 200\ M^{-1}$ was obtained (Figure 8).

The equilibrium constant K_T, for the interconversion between the hemiacetal (B) and the *E*-chalcone (C_E), is not affected by the aggregation or copigmentation reactions; therefore, it can be obtained from the representation of $[C_E]$ as a function of [B] ($[C_E] = K_T[B]$). This was done using all data points (for the three initial concentrations) in the same plot, and a value of $K_T = 0.26 \pm 0.01$ was obtained from the slope.

The apparent hydration constant, K_h^{app}, can be obtained in a similar way by the representation of $[B]/[AH^+]_{app}$ as a function of $1/[H^+]$ ($[B]/[AH^+]_{app} = K_h^{app}/[H^+]$), but as $[AH^+]_{app}$ includes the contributions of [D] and $[AHC_Z^+]$, K_h^{app} depends on the initial concentration. It can be shown (see Appendix) that the reciprocal value of K_h^{app} is linearly dependent on the initial concentration (C_0) for a given pH value. The slope is a complex function of the equilibrium constants and the *y*-axis intercept is equal to the reciprocal K_h value. From the plot of $1/K_h^{app}$ vs C_0, a value of $K_h = 0.0016 \pm 0.0008$ is obtained.

In the same way, the representation of $[C_Z]_{app}$ as a function of $[C_E]$ yields several values of K_i^{app}, which when plotted against C_0, give a straight line from which the value of $K_i = 0.6 \pm 0.1$ (*y*-axis intercept) was obtained.

Furthermore, the concentrations of the several species in eqs 1−5 can be expressed as functions of the equilibrium constants, the hydrogen ion concentration, and the total concentration of anthocyanin (eqs 7 to 14).

$$C_0 = \beta[AH^+]^2 + \alpha[AH^+] \tag{7}$$

with,

$$\alpha = 1 + \frac{K_h}{[H^+]} + \frac{K_hK_T}{[H^+]} + \frac{K_hK_TK_i}{[H^+]} \tag{8}$$

and

$$\beta = 2\left(K_d + \frac{K_{cop}K_hK_TK_i}{[H^+]}\right) \tag{9}$$

$$[B] = K_h[AH^+]/[H^+] \tag{10}$$

$$[C_E] = K_hK_T[AH^+]/[H^+] \tag{11}$$

$$[C_Z] = K_hK_TK_i[AH^+]/[H^+] \tag{12}$$

$$[D] = K_d[AH^+]^2 \tag{13}$$

$$[AHC_Z^+] = K_{cop}K_hK_TK_i[AH^+]^2/[H^+] \tag{14}$$

Equations 7−14 can be used to analyze the data shown in Figure 3 in order to estimate the copigmentation constant and to check the interconsistency of the previously determined constants, as described below.

Determination of Equilibrium Constants from Molar Fractions vs pH Plots. The model presented above was tested in two steps: first, only self-association was considered; i.e., K_{cop} was set equal to zero in eqs 7 through 14. Accordingly, the flavylium concentration determined from NMR data was equated to the sum of concentrations of all species where AH^+ is present, weighted for the number of equivalent protons:

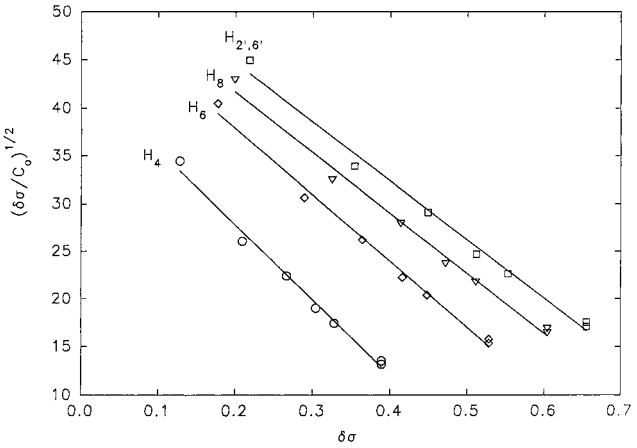

Figure 8. Plots of Dimicoli and Hélène's equation to determine the self-aggregation constant of the flavylium cation form of malvidin 3-glucoside at pH = 0.8.

$$[AH^+]_{tot} = [AH^+] + 2[D] \tag{15}$$

In a second step, both association processes were included; i.e., the apparent concentrations of flavylium $[AH^+]_{tot}$, and *Z*-chalcone, $[C_Z]_{tot}$, are given by:

$$[AH^+]_{tot} = [AH^+] + 2[D] + [AHC_Z^+] \tag{16}$$

and

$$[C_Z]_{tot} = [C_Z] + [AHC_Z^+] \tag{17}$$

Equations 7 through 17 were employed to fit the pH dependence of the experimental molar fractions (previously shown in Figure 3), using the equilibrium constants as fitting parameters.

In the first analytical approach (inclusion of self-association alone), the apparent K_h change was correctly described, but poor fits were obtained, namely, (i) the pH dependence of AH^+ and C_Z molar fractions could not be adjusted in the full pH range and (ii) the experimentally observed inversion of the relative values of the C_Z and C_E molar fractions (Figure 3c) could not be predicted. Also, further addition of the $AH^+ \leftrightarrow A$ equilibrium did not significantly improve the quality of the fits. When both the dimerization and copigmentation processes were considered, these difficulties were removed, although independent fitting of each of the three sets of data gave multiple solutions, indicating that the signal-to-noise ratio of the data was insufficient to define the absolute minimum in the multidimensional error surface when all equilibrium constants were allowed to change. To overcome this problem, the values for K_h, K_T, and K_i (using the values found above) had to be fixed and the fitting was made using only K_d and K_{cop} as variable parameters. The values of K_d obtained in this manner were higher than those predicted by the Dimicoli−Hélène relation and showed a strong dependence of the initial concentration (see Table 2). Similar dependence on the initial concentration was found for K_{cop}, but while K_{cop} was critically dependent on small changes in the value of K_d, this latter constant was insensitive to small changes in the value of K_{cop}. Therefore, an independent determination of this constant was necessary.

Determination of K_{cop} from NMR Chemical Shifts as f(pH). Extension of the Dimicoli−Hélène Method. The observed chemical shifts of the *Z*-chalcone H_4 and $H_{2'+6'}$ protons,

TABLE 2: K_d Values Obtained from Global Fitting of Molar Fractions (Figure 3) to Equations 7−14 and 16−17, and K_{cop} Values Obtained from Data in Figure 9

C_0	K_d	K_{cop}
0.14 mM	4440	3560
0.42 mM	7340	4700
0.68 mM	17130	8000

δ_{CZ}, can be related to the chemical shifts of C_Z and AHC_Z^+ in the absence of exchange, (δ^0_{CZ} and δ^0_{AHCZ}, respectively) by eq 18:

$$\delta_{Cz} = \frac{\delta^0_{C_z}[C_Z] + \delta^0_{AHC_z}[AHC_Z^+]}{[C_Z] + [AHC_Z^+]} \tag{18}$$

which can be rearranged to obtain a linear relationship between the reciprocal chemical shift change ($\Delta = \delta_{CZ} - \delta^0_{CZ}$) and the reciprocal concentration of hydrogen ion times the molar fraction of hemiacetal (eq 19).

$$\frac{1}{\Delta} = \frac{1}{\Delta^0}\left(1 + \frac{K_h}{K_{cop}} \times \frac{1}{X_B[H^+]}\right) \tag{19}$$

Since $\Delta^0 = \delta^0_{AHC_Z} - \delta^0_{C_Z}$ is constant for a given proton, plots of $1/\Delta$ as a function of $1/\{X_B[H^+]\}$, where X_B is the hemiacetal molar fraction, measured with solutions with different initial concentrations (C_0), should give the same straight line with intercept $1/\Delta^0$ and slope $K_h/\Delta^0 K_{cop}$. Such plots (Figure 9) clearly show that the slopes depend on the initial concentration, C_0, and consequently the copigmentation constant obtained in this way also shows a strong dependence of the initial concentration (Table 2) as found in the fittings for K_d and K_{cop}. This led us to the conclusion that the assumed model does not correctly describe the equilibria in solution. The fit of the experimental molar fractions with $K_h = 0.0016$, $K_T = 0.26$, $K_i = 0.6$, and the concentration-dependent values of K_d and K_{cop} (Table 2) are shown in Figure 3 (lines).

Model Including Multi-Aggregation. It is clear that if we assume that both the self-aggregation and copigmentation reactions will produce only dimers, in the presence of multi-aggregates the obtained dimerization constants are just apparent constants and will depend on the initial concentration.

In the case of flavylium self-aggregation, if we assume n aggregation steps and the simplifying approximation that the association constant (K) has the same value for each step, we will have the following scheme:

$$M + M \overset{K}{\rightleftharpoons} M_2$$

$$M + M_2 \overset{K}{\rightleftharpoons} M_3$$

$$\vdots$$

$$M + M_{n-1} \overset{K}{\rightleftharpoons} M_n$$

where M stands for the flavylium cation, M_2 for the dimer, and M_n for the aggregate constituted by n flavylium molecules. A simple relation between K_d and K can be derived (eq 20) and from a plot of $1/K_d$ vs C_0 (see Appendix), $1/K$ is obtained from the y-axis intercept (Figure 10).

$$\frac{1}{K_d} = \frac{1}{K} - [M] \tag{20}$$

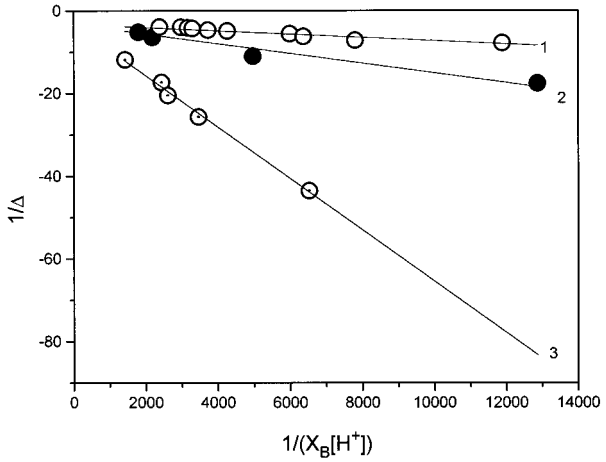

Figure 9. Plots of $1/\Delta$ vs $1/(X_B[H^+])$ (eq 19); line 1: $C_0 = 0.68$ mM; line 2: $C_0 = 0.42$ mM; line 3: $C_0 = 0.14$ mM.

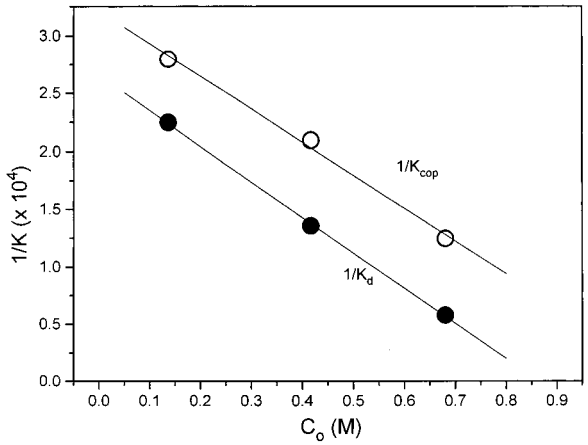

Figure 10. Plots of $1/K_d$ and $1/K_{cop}$ vs C_0.

In the same way, it can be shown that, for the copigmentation process of the oligomers [in order to avoid unnecessary complexity and given the fact that there is no C_Z self-aggregation, mixed order aggregates of the form M_nC_{Zm} with $m > 1$ are not considered], the apparent constant, K_{cop}, is related to the real constant, K' (also assumed to be the same for each of the n steps), as follows (see Appendix):

$$M + C_Z \overset{K'}{\rightleftharpoons} MC_Z$$

$$M_2 + C_Z \overset{K'}{\rightleftharpoons} M_2C_Z$$

$$\vdots$$

$$M_n + C_Z \overset{K'}{\rightleftharpoons} M_nC_Z$$

$$\frac{1}{K_{cop}} = \frac{1}{K'} - \frac{K}{K'}[M] \tag{21}$$

And by the same argument it is possible to obtain K' from the plot of $1/K_{cop}$ vs C_0. The plots of $1/K_d$ and $1/K_{cop}$ as a function of C_0, shown in Figure 10, are linear and give values of $K = 3700$ and $K' = 3030$.

The self-aggregation constant in the case of the formation of multi-aggregates can also be obtained from the Dimicoli−Hélène methodology,[13] using the following equation:

$$\left(\frac{\delta}{C_0}\right)^{1/2} = \left(\frac{K}{2\delta\sigma_{C_2}}\right)^{1/2}(2\delta\sigma_{C_2} - \delta\sigma) \qquad (22)$$

where K is now the equilibrium constant for each step of aggregation, considered equal for all n steps, C_0 is the total concentration of pigment, $\delta\sigma$ is the difference between extrapolated chemical shift at infinite dilution and actual chemical shift at a given concentration, $\delta\sigma_{C_2}$ is the difference between the chemical shift of the aggregates (obviously the mean value of the shifts of all aggregates weighted by the respective molar fractions) and the actual chemical shift. Under these conditions (multi-aggregation), K can be calculated from the plot shown in Figure 8 where the x-axis intercept is now $2\delta\sigma_{C_2}$ and the slope $(K/2\delta\sigma_{C_2})^{1/2}$. A value of $K = 3600 \pm 400\ M^{-1}$ was obtained, in excellent agreement with that obtained from Figure 10.

Concluding Remarks

The experimental evidence clearly points to the existence of copigmentation processes between two of the existent malvidin 3-glucoside forms in aqueous solution: the flavylium cation and the *Z*-chalcone. From a global analysis of the data, including the initial concentration and the pH dependence of the molar fractions and the chemical shifts, it was possible to conclude that copigmentation and self-aggregation are multi-aggregation processes. The different ability for aggregation of the two chalcone isomers is compatible with the more planar structure expected for the *Z* isomer when compared to the *E* isomer, the planar structure favoring closer packing with the flavylium cation.

In addition to the previously reported self-aggregation of the flavylium cation, which leads to color stabilization at very acidic pH values, the process of copigmentation of the flavylium cation with the *Z*-chalcone, here described for the first time, opens a wide range of possibilities that result in color stabilization by natural chalcones at less acidic pH values. It is very likely that this process may have a relevant contribution to the well-known stability of the flavylium cation observed in the original systems, i.e., in plant cells and in wine.

Appendix

***K_h^{app}* as Function of *C_0*.** The apparent hydrolysis constant is defined as:

$$K_h^{app} = \frac{[B][H^+]}{[AH^+]_{app}} = \frac{[B][H^+]}{[AH^+] + 2[D] + [AHC_Z{}^+]} \qquad (A1)$$

and its reciprocal can be expressed as a function of $[AH^+]$ using eqs 9, 10, 13, and 14 to yield:

$$\frac{1}{K_h^{app}} = \frac{1}{K_h} + \frac{1}{K_h}\left(k_d + \frac{\beta}{2}\right)[AH^+] \qquad (A2)$$

$[AH^+]$ is equal to C_0/α when $[AH^+] \ll \alpha/\beta$, (see eq 7) under which condition:

$$\frac{1}{K_h^{app}} = \frac{1}{K_h} + \frac{1}{\alpha K_h}\left(k_d + \frac{\beta}{2}\right)C_0 \qquad (A3)$$

The limit of $1/K_h^{app}$ when $C_0 \to 0$ is equal to $1/K_h$.

***K_i^{app}* as Function of *C_0*.** If K_i^{app} is defined as

$$K_i^{app} = \frac{[C_Z]_{app}}{[C_E]} = \frac{[C_Z] + [AHC_Z{}^+]}{[C_E]} \qquad (A4)$$

substitution with eqs 11, 12, and 14 leads to:

$$K_i^{app} = K_i + K_i K_{cop}[AH^+] \qquad (A5)$$

or , when $[AH^+] \ll \alpha/\beta$, to:

$$K_i^{app} = K_i + \frac{K_i K_{cop}}{\alpha}C_0 \qquad (A6)$$

and K_i is obtained from $\lim_{C_0 \to 0} K_i^{app}$.

***K_d* as Function of *C_0*.** In the expression that describes the apparent dimerization constant ($K_d = [D]/[AH^+]^2$), [D] stands for the distribution of all the oligomers in solution whose concentrations are now described as a function of the equilibrium constant, K:

$$[D] = [M_2] + \frac{3}{2}[M_3] + ... + \frac{n}{2}[M_n] = [M_2]\left(K + \frac{3}{2}K^2[M] + ... + \frac{n}{2}K^{n-1}[M]^{n-2}\right) \qquad (A7)$$

or simply,

$$[D] = K[M]^2\sum_{i=2}^{n}\left(\frac{i}{2}K^{i-1}[M]^{i-2}\right) \qquad (A8)$$

The apparent constant K_d can now be described as a function of the new definition derived for [D]:

$$K_d = \frac{[D]}{[M]^2} = K\sum_{i=2}^{n}\left(\frac{i}{2}K^{i-1}[M]^{i-2}\right) \qquad (A9)$$

Since this series is the derivative of a power series one readily obtains, when $K[M] < 1$ and $n \to \infty$:

$$K_d = \frac{K}{1 - K[M]} + \frac{K^2[M]}{2(1 - K[M])^2} \qquad (A10)$$

Furthermore, the second term in the right side becomes negligible when $K[M] < 2/3$, and eq A10 reads:

$$\frac{1}{K_d} = \frac{1}{K} - [M] \qquad (A11)$$

or, when $[AH^+] \ll \alpha/\beta$:

$$\frac{1}{K_d} = \frac{1}{K} - \frac{C_0}{a} \qquad (A12)$$

and $\lim_{C_0 \to 0} 1/K_d = 1/K$.

***K_{cop}* as Function of *C_0*.** When $[AHC_Z{}^+]$ is defined as the sum of concentrations of all the copigments of the oligomers:

$$[AHC_Z{}^+] = [MC_Z] + [M_2C_Z] + ... + [M_nC_Z] = K'[M][C_Z] + K'[M_2][C_Z] + ... + K'[M_n][C_Z] \qquad (A13)$$

one obtains:

$$K_{cop} = \frac{[AHC_Z{}^+]}{[M][C_Z]} = K'\sum_{i=0}^{n}(K[M])^i \qquad (A14)$$

or, when $K[M] < 1$ and $n \rightarrow \infty$:

$$K_{cop} = \frac{K'}{1 - K[M]} \tag{A15}$$

Also, when $[AH^+] \ll \alpha/\beta$:

$$\frac{1}{K_{cop}} = \frac{1}{K'} - \frac{K}{K'}[M] = \frac{1}{K'} - \frac{K}{aK'}C_0 \tag{A16}$$

and $\lim_{C_0 \rightarrow 0} 1/K_{cop} = 1/K$.

The convergence condition of eqs A9 and A14 ($K[M] < 1$), as well as the condition $K[M] < 2/3$, are satisfied for all data points ((C_0, pH) pairs) ($[M]_{max} = 0.14$ mM for $C_0 = 0.42$ mM and pH = 1).

The condition of direct proportionality between $[AH^+]$ and C_0, ($[AH^+] \ll \alpha/\beta$) leading to eqs A3, A6, A12, and A16 is satisfied for all pH values when $C_0 = 0.14$ mM. When $C_0 = 0.42$ mM and $C_0 = 0.68$ mM, the condition is strictly satisfied only for pH values larger than 3 and 3.5, respectively. However, consideration of either all data or only those satisfying the linearity condition leads to the same intercept values.

References and Notes

(1) Brouillard, R. In *Anthocyanins as Food Colors*; Markakis, P., Ed.; Academic Press: New York, 1982; Chapter 9.

(2) Brouillard, R. *Phytochemistry* **1981**, *20*, 143.

(3) Brouillard, R.; Dubois, J.-E. *J. Am. Chem. Soc.* **1977**, *99*, 1359.

(4) Brouillard, R.; Delaporte, B.; Dubois, J.-E. *J. Am. Chem. Soc.* **1978**, *100*, 6202.

(5) Cheminat, A.; Brouillard, R. *Tetrahedron Lett.* **1986**, *27*, 4457.

(6) Goto, T.; Kondo, T. *Angew. Chem., Int. Ed. Engl.* **1991**, *30*, 17.

(7) Asen, S.; Stewart, R. N.; Norris, K. H. *Phytochemistry* **1972**, *11*, 1139.

(8) Hoshino, T.; Matsumoto, U.; Harada, N.; Goto, T. *Tetrahedron Lett.* **1981**, *22*, 3621.

(9) Hoshino, T.; Matsumoto, U.; Harada, N. Goto, T. *Phytochemistry* **1981**, *20*, 1971.

(10) Hoshino, T.; Matsumoto, U.; Harada, N.; Goto, T. *Tetrahedron Lett.* **1982**, *23*, 433.

(11) Hoshino, T. *Phytochemistry* **1991**, *30*, 2049.

(12) Hoshino, T. *Phytochemistry* **1992**, *31*, 647.

(13) Dimicoli, J.-L.; Hélène, C. *J. Am. Chem. Soc.* **1973**, *95*, 1036.

(14) Nerdal, W.; Andersen, Ø. M. *Phytochem. Anal.* **1991**, *2*, 263.

(15) Nerdal, W.; Andersen, Ø. M. *Phytochem. Anal.* **1992**, *3*, 182.

(16) Mazza, G.; Brouillard, R. *Food Chem.* **1987**, *27*, 207.

(17) Mistry, T. V.; Cai, Y.; Lilley, T. H.; Haslam, E. *J. Chem. Soc., Perkin Trans.* **1991**, *2*, 1287.

(18) Dangles, O.; Saito, N.; Brouillard, R. *J. Am. Chem. Soc.* **1993**, *115*, 3125.

(19) Saito, N.; Tatsuzawa, F.; Nishiama, A.; Yokoi, M.; Shigihara, A.; Honda, T. *Phytochemistry* **1995**, *38*, 1027.

(20) Saito, N.; Tatsuzawa, F.; Yoda, K.; Yokoi, M.; Kasahara, K.; Iida, S.; Shigihara, A.; Toshio Honda, T. *Phytochemistry* **1995**, *40*, 1283.

(21) Figueiredo, P.; Elhabiri, M.; Saito N.; Brouillard, R. *J. Am. Chem. Soc.* **1996**, *118*, 4788.

(22) Santos, H.; Turner, D. L.; Lima, J. C.; Figueiredo, P.; Pina, F.; Maçanita, A. L. *Phytochemistry* **1993**, *33*, 1227.

(23) Rüedi, P.; Hutter-Beda, B. *Bull. Liaison Group Polyphenols* **1990**, *15*, 332.

(24) Becker, R. S. *Theory and Interpretation of Fluorescence and Phosphorescence*; Wiley Interscience: New York, 1969.